

Effect of an amorphous TiO₂ addition on dye-sensitized solar cells with organic dyes

Nariaki Kakuta, Takeo Oku*, Atsushi Suzuki, Kenji Kikuchi and Shiomi Kikuchi

Department of Materials Science, The University of Shiga Prefecture, Hassaka 2500, Hikone, Shiga 522-8533, Japan

Dye-sensitized solar cells with organic dyes of xylanol orange and rose bengal were fabricated and characterized. A solar cell with mixed xylanol orange and rose bengal showed a higher conversion efficiency compared to solar cells with one type of dye. In addition, amorphous TiO₂ layers were introduced to attract electrons, which were mixed phases of anatase and amorphous. The current density was improved by the TiO₂ layer introduced, and the conversion efficiency increased.

Key words: Solar cell, Dye-sensitized, Amorphous TiO₂.

Introduction

Solar cells are clean energy devices that provide electricity, and produce no carbon dioxide semi-permanently and hazardous waste gases causing global warming. Silicon (Si) solar cells have a high conversion efficiency and a long lifetime. However, production processes are complicated, and the cost is high. Dye-sensitized solar cells, which are based on the concept of photo-sensitization of wide band gap mesoporous oxide semiconductors, are now in a state of advanced development. This technology has been established as a promising low-cost photovoltaic concept and was recently improved to be near 11% efficient [1]. In the case of using a single dye, the maximum theoretical efficiency is expected to be 33% although cell performance is improved by combining with other dyes [2-3] In addition, dye-sensitized solar cells have featured applications that can be colored and are lightweight. However, dye-sensitized solar cells have a short lifetime due to leakage and evaporation of the electrolytes. Therefore, studies of solidification of dye-sensitized solar cells have been performed actively [4-5]. Organic dyes attract attention as cheap dyes without noble metals.

The purpose of the present study was to investigate the electrical and optical properties of dye-sensitized solar cells, with amorphous TiO₂ to attract electrons at trap levels in the acceptor and donor levels. In a previous study, the effects of the addition of organic dyes such as XO and RB to dye-sensitized solar cells on the electrical and optical properties have been investigated [6] Xylanol orange (XO) and rose Bengal (RB) have been studied as organic dyes [7-8].

Experimental

Nanocrystalline TiO₂ photoelectrodes were prepared using

the following procedure. TiO₂ powder was dispersed in an aqueous solution (1 ml) litre in a mixture of acetylacetone (0.02 ml, Shigma Aldrich Inc.) with Triton X-100 (0.01 ml, ICN Biomedicals Inc.) with polyethylene glycol (0.2 g, PEG#20,000, Nacalai Tesque Co. Ltd.) [9] The TiO₂ paste was coated on pre-cleaned F-doped SnO₂ (FTO, A11DU80, AGC Fabritech Co. Ltd.) coated glass substrates by the squeegee method. After the TiO₂ coating, the FTO substrate was sintered for 30 minutes at 450 °C, and the prepared TTIP solution dropped on the substrate. After that, the substrate was sintered for 1 hour at 180 °C. The TTIP solution was prepared by mixing titanium isopropoxide (TTIP, 0.3 ml, Sigma Aldrich Co. Ltd.), acetilaceton (0.08 ml), ethanol (0.64 ml) and PEG (#2,000, 0.2 g, Nacalai Tesque Co. Ltd.). The TiO₂ electrodes were dissolved into the solved organic dyes such as xylanol orange and rose bengal solutions (Tokyo Chemical Industry Co. Ltd.) in distilled water, methanol or ethanol (Nacalai Tesque Co. Ltd.). Bellfine (0.1 g, Air water Inc.) and Denka black (0.02 g, Denki kagaku kogyo Co. Ltd.) as carbon was dispersed in the distilled water (0.8 ml) and ethanol (0.4 ml) with sodium carboxymethyl cellulose (0.012 g, Tokyo Chemical Industry Co. Ltd.) [10] The carbon paste was applied on indium tin oxide (ITO, Geomatec Co. Ltd.) as an opposite electrode by the squeegee method. The heat treatment of the carbon on the ITO substrate was carried out at 180 °C for 30 minutes. The electrolyte fabricated in a mixture of iodine (I₂, 0.05 g, Wako Co. Ltd.), lithium iodide (LiI, 0.09 g, Wako Co. Ltd.), ethylene carbonate (EC, 0.41 g, Shigma Aldrich Inc.), propylene carbonate (PC, 0.5 ml, Shigma Aldrich Inc.) and polyacrylonitrile (PAN, 0.17 g, Shigma Aldrich Inc.) was agitated and heated at 80 °C [11] The dye-sensitized solar cells were assembled by putting the electrolyte between the adsorbed dye materials at the TiO₂ layer on the FTO glass substrate and the carbon film on the ITO substrate.

Light and dark current density voltage J-V characteristics (Hokuto Co. Ltd.) were measured under AM 1.5 (100 mWcm⁻²) irradiation. The optical properties of UV-vis spectroscopy of dye-sensitized solar cells were measured

*Corresponding author:
Tel : +81-749-28-8368
Fax: +81-749-28-8590
E-mail: oku@mat.usp.ac.jp

by UV-vis spectroscopy (Hitachi U-4100). Transmission electron microscopy (TEM) observations with electron diffraction patterns regarding the TiO_2 particles was carried out by a 200 kV TEM (Hitachi H-8100). The crystal structure of the TiO_2 was investigated by X-ray diffraction (X'Pert-MPD system Philips Co. Ltd.) using $\text{CuK}\alpha$ radiation. The crystal indices were analyzed on the basis of the crystal database. The surface structure of sintered TiO_2 films was observed by scanning electron microscope (SEM, HITACHI S-3200N).

Results and Discussion

Measured J-V characteristics of a DSSC with an amorphous TiO_2 layer are shown in Fig. 1. The current density of DSSC with an amorphous TiO_2 layer was higher than that of DSSC without an amorphous TiO_2 layer. The cell performance is summarized as Table 1. The current density was improved from 0.6 mA/cm^2 to 0.83 mA/cm^2 . The other parameters are almost the same. As a result, the conversion efficiency was improved from 0.12% to 0.16%.

Fig. 2 shows the measured optical absorption of DSSC with an amorphous TiO_2 layer compared to that without an amorphous TiO_2 layer. An optical absorption peak of TiO_2 around 380 nm is increased by introducing the amorphous TiO_2 layer, which is due to the anatase phase including amorphous TiO_2 .

Fig. 3 show SEM images of the surface and cross-section of TiO_2 layers. From the SEM image of the surface, the TiO_2 layer is covered overall with the amorphous TiO_2 layer. Film thicknesses are $\sim 17 \mu\text{m}$ for both samples

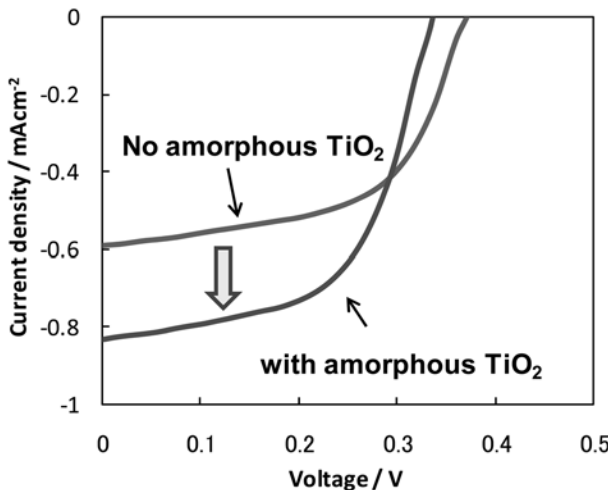


Fig. 1. J-V characteristics of DSSCs with or without an amorphous TiO_2 layer.

Table 1. Comparison of parameters of DSSCs

	V_{OC} (V)	J_{SC} (mA/cm^2)	FF	η (%)
No amorphous TiO_2 layer	0.36	0.60	0.56	0.12
With amorphous TiO_2 layer	0.33	0.83	0.58	0.16

from cross-sectional images.

Fig. 4 shows a TEM image and an electron diffraction pattern of the amorphous TiO_2 layer. An amorphous TiO_2 layer around the TiO_2 nanoparticle was observed in the TEM image. As shown in Fig. 4(b), the electron diffraction pattern indicates 101 and 103 reflections of the polycrystalline coagulation of TiO_2 with a tetragonal anatase structure. Diffuse ring of the amorphous phase was also

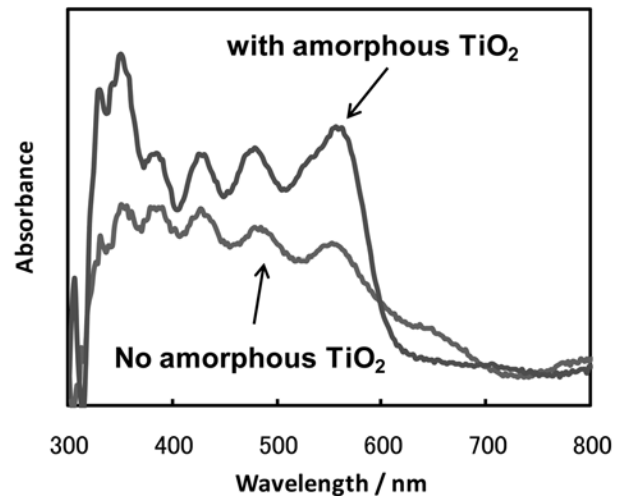


Fig. 2. Optical absorption of DSSCs with or without an amorphous TiO_2 layer.

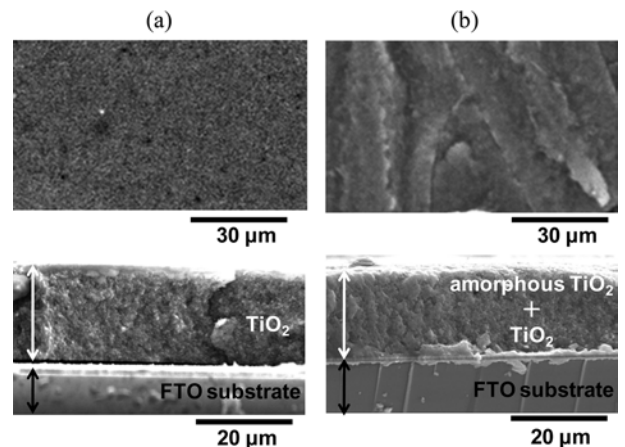


Fig. 3. SEM images of surface and cross-section of (a) amorphous TiO_2 layer and (b) no amorphous TiO_2 layer, respectively.

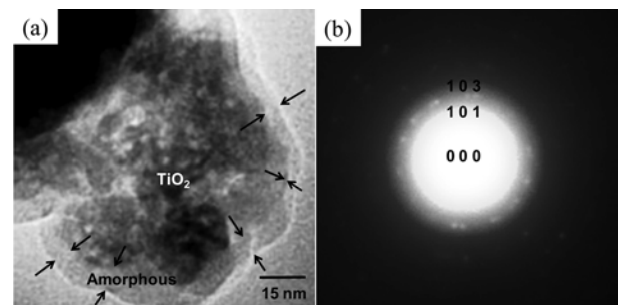


Fig. 4. (a) TEM image and (b) electron diffraction pattern of an amorphous TiO_2 layer.

observed, which indicates the structure of the TiO_2 layer introduced was a mixture phase of anatase and amorphous.

Fig. 5 shows X-ray diffraction patterns of TiO_2 layers prepared from the TTIP solution as a function of temperature. No peak of the anatase was observed when annealing at 250 °C. Small peaks of the anatase phase were observed after annealing at 350 °C. Peaks of TiO_2 (P25) are shown as comparison of the amorphous TiO_2 .

An energy level diagram of DSSC with the amorphous TiO_2 layer is summarized in Fig. 6. The values of HOMO and LUMO were calculated by a Gaussian03 (B3LYP, 6-31G*). An energy barrier would exist at the semiconductor metal interface. Electronic charge-transfer separation was caused by light irradiation from the FTO substrate side. The TiO_2 layer or amorphous TiO_2 layer accepts the electrons from the dye, and the electrons are attracted by several trap levels of the amorphous TiO_2 . Electrons are transported to an FTO electrode through the TiO_2 layer, and electrons drift

to the outside circuit, and flow through the carbon electrode. Additionally, electrons are returned by the oxidation-reduction reaction of the electrolyte. Control of the energy levels is important to increase the efficiency.

Carrier recombination would be a main cause to yield a low conversion efficiency. The improvement of the conversion efficiency can be expected by improving the charge separation and the electronic charge transfer. The improvement of the present solar cells is thought to be by the introduction of the amorphous TiO_2 electrode, and this structure should be investigated further.

Improvements of the conversion efficiency by coating materials on TiO_2 have been reported. Insulator oxides such as Al_2O_3 or SiO_2 on TiO_2 have been introduced for DSSCs [12]. These oxides inhibit the carrier recombination by reverse transfer of electrons in the cells. In the present study, DSSCs with amorphous TiO_2 layers on TiO_2 were fabricated, and the amorphous TiO_2 would attract electrons because there are many trap levels in the acceptor and donor levels. In addition, the effectiveness of carrier separation is high since the contact area is large.

Conclusions

Amorphous TiO_2 was introduced into DSSC with mixed xylenol orange and rose Bengal. The optical absorption peak of TiO_2 around 380 nm was increased by introducing the amorphous TiO_2 layer. Diffraction spots of the anatase phase and a diffuse ring from the amorphous phase were observed in the TEM observations. The proposed energy diagram shows the amorphous TiO_2 would attract electrons due to several trap levels in the acceptor and donor. In addition, the effectiveness of carrier separation is high since the contact area is large. As a result, the current density was improved from 0.60 mA/cm² to 0.83 mA/cm², and the conversion efficiency was improved from 0.12% to 0.16%.

References

- M. Durr, A. Bamedi, A. Yasuda and G. Nellesa, *Appl. Phys. Lett.* 84 (2004) 3397-3399.
- H.-J. Koo, K. Kim, N.-G Park, S. Hwang, C. Park and C. Kim, *Appl. Phys. Lett.* 92 (2008) 142103-1-3.
- F. Inakazu, Y. Noma, Y. Ogomi and S. Hayase, *Appl. Phys. Lett.* 93 (2008) 093304-1-3.
- S. Murai, S. Mikoshiba and S. Hayase, *Sol. Energy Mater. Sol. Cells* 91 (2007) 1707-1712.
- L. Schmidt-Mende, U. Bach, R. Humphry-Baker, T. Horiuchi, H. Miura, S. Ito, S. Uchida and M. Gratzel, *Adv. Mater.* 17 (2005) 813-815.
- B. Pradhana, S.K. Batabyal and A.J. Pal, *Sol. Energy Mater. Sol. Cells* 91 (2007) 769-773.
- N. Kakuta, T. Oku, A. Suzuki, K. Kikuchi and S. Kikuchi, *J. Ceram. Soc. Jpn.* 117 (2009) 964-966.
- T. Matsubara, Y. Ichikawa, K. Aramaki and A. Katagiri, *Sol. Energy Mater. Sol. Cells* 85 (2005) 269-275.
- M.K. Nazeeruddin, A. Kay, I. Rodicio, R. Humphry-Baker, E. Muller, P. Liska, N. Vlachopoulos and M. Gratzel, *J. Am. Chem. Soc.* 115 (1993) 6382-6390.

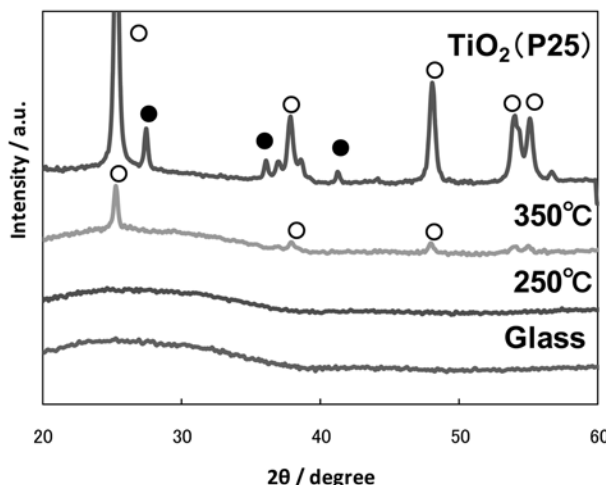


Fig. 5. X-ray diffraction patterns of TiO_2 layers as a function of temperature. (○ : anatase ● : rutile)

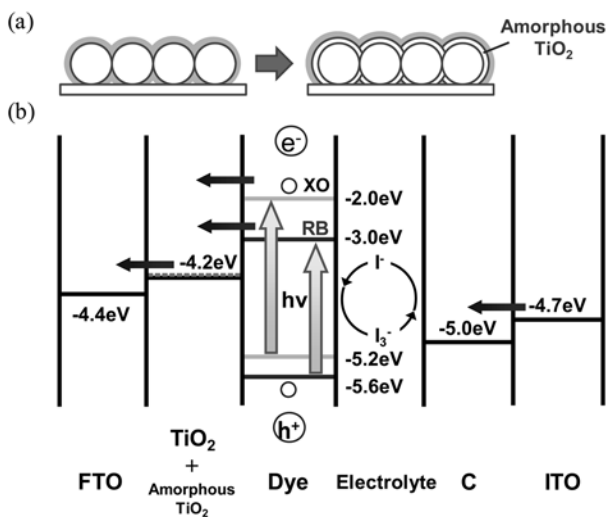


Fig. 6. (a) Schematic diagram of TiO_2 electrode with an amorphous TiO_2 layer. (b) Energy level diagram of the present DSSC with amorphous TiO_2 layers.

10. K. Imoto, K. Takahashi, T. Yamaguchi, T. Komura, J. Nakamura and K. Murata, Sol. Energy Mater. Sol. Cells 79 (2003) 459-469.
11. O.A. Ileperuma, M.A.K.L. Dissanayake, S. Somasunderam and L.R.A.K. Bandara, Sol. Energy Mater. Sol. Cells 84 (2004) 117-124.
12. E. Palomares, J.N. Clifford, S.A. Haque, T. Lutz and J.R. Durrant, J. Am. Chem. Soc. 125 (2003) 475-482.